Acta Oceanol. Sin., 2022, Vol. 41, No. 6, P. 78–87
https://doi.org/10.1007/s13131-021-1894-z
http://www.aosocean.com
E-mail: ocean2@hyxb.org.cn

Two drifting paths of *Sargassum* bloom in the Yellow Sea and East China Sea during 2019–2020

Chao Yuan[1, 2, 3], Jie Xiao[1, 2], Xuelei Zhang[1, 2, 3*], Mingzhu Fu[1, 2], Zongling Wang[1, 2*]

[1] The MNR Key Laboratory of Marine Eco-Environmental Science and Technology, First Institute of Oceanography, Ministry of Natural Resources, Qingdao 266061, China

[2] Laboratory of Marine Ecology and Environmental Science, Pilot National Laboratory for Marine Science and Technology (Qingdao), Qingdao 266237, China

[3] National Engineering Laboratory for Integrated Aero-Space-Ground-Ocean Big Data Application Technology, Xi'an 710129, China

Received 26 March 2021; accepted 15 June 2021

Abstract

The macroalgal blooms of floating brown algae *Sargassum horneri* are increasing in the Yellow Sea and East China Sea during the past few years. However, the annual pattern of *Sargassum* bloom is not well characterized. To study the developing pattern and explore the impacts from hydro-meteorologic environment, high resolution satellite imageries were used to monitor the distribution, coverage and drifting of the pelagic *Sargassum* rafts in the Yellow Sea and East China Sea from September 2019 to August 2020. *Sargassum* blooms were detected from October 2019 to June 2020 and presented two successive drifting paths that both initiated from around 37°N. The first path spanned smaller spatial scale and shorter period, starting with a bloom of 3 km^2 distribution area near the eastern tip of Shandong Peninsula in late October 2019 and drifted southwards, hit the *Pyropia* aquaculture area in early January 2020, then vanished in the northwest of East China Sea (ca. 32°N) around end of January. The second path began with a large distribution area of 23 000 km^2 east of 123°E in late January 2020, firstly moved southwards in the central Yellow Sea and northern East China Sea (north of 29°N) till late April, then turned northwards with monsoon wind and vanished from late June to August. The mean sea surface temperature of 8°C to 20°C in the *Sargassum* bloom areas corresponded to *in situ* observed temperature range for vegetative growth and floating of *S. horneri*. There was no observed floating *Sargassum* blooms during July through September in the Yellow Sea and East China Sea. The results indicate that floating *S. horneri* is unable to complete life cycle in the Yellow Sea and East China Sea, and provide insights to the future management of *Sargassum* blooms. Further studies are needed to validate the pattern and source of annual *Sargassum* bloom in the Yellow Sea and East China Sea.

Key words: *Sargassum horneri*, macroalgal bloom, high resolution remote sensing, wind directions, sea surface temperature, Yellow Sea and East China Sea

Citation: Yuan Chao, Xiao Jie, Zhang Xuelei, Fu Mingzhu, Wang Zongling. 2022. Two drifting paths of *Sargassum* bloom in the Yellow Sea and East China Sea during 2019–2020. Acta Oceanologica Sinica, 41(6): 78–87, doi: 10.1007/s13131-021-1894-z

1 Introduction

Seaweed blooms, mass stranding of macroalgae along the coasts, are increasing worldwidely during the past few decades and become nauseant ecological disasters in some coastal regions. Two genera, green algae *Ulva* and brown algae *Sargassum*, are responsible for most seaweed blooms, namely "green" and "golden" tides, respectively (Smetacek and Zingone, 2013). The inundation of huge seaweed biomasses along the coasts could seriously harm tourism, aquaculture, fisheries and marine ecosystems (Smetacek and Zingone, 2013; Wang et al., 2015, 2019; Xing et al., 2017; Byeon et al., 2019). Recently, blooms of *Ulva prolifera* O. F. Müller, 1778 and *Sargassum horneri* (Turner) C. Agardh, 1820 co-occurred in the Yellow Sea (YS) and formed an unusual bi-macroalgal bloom (Xiao et al., 2020a and b, 2021b). Extensive studies have been conducted in the YS and revealed consistent genesis and development process of the green tides (Liu et al., 2010; Cui et al., 2012; Fan et al., 2015; Song et al., 2015a, b; Wang et al., 2015; Xing et al., 2018; Xiao et al., 2020a). However, little is known about the formation and development of golden tides in the YS and East China Sea (ECS).

The golden tides along the eastern Chinese coasts are comprised almost exclusively of *S. horneri* (Liu et al., 2018; Xing et al., 2018). *S. horneri* is an introduced regional species naturally distributing along the northwestern Pacific coast and has invaded the coasts of southern California and Mexico along the eastern Pacific in early 2000s (Tseng, 1983; Sun et al., 2008; Marks et al., 2015; Darling and Carlton, 2018). The gas-filled bladder-like vesicles on the thalli of *S. horneri* provide buoyancy to float in water (Yoshida, 1963; Xu et al., 2016). Free-floating *S. horneri* is common in the coastal waters of northwestern Pacific (Komatsu et al.,

Foundation item: The National Key Research and Development Program of China under contract No. 2016YFC1402100; the National Natural Science Foundation of China under contract No. 41876137; the Marine S&T Fund of Shandong Province for Pilot National Laboratory for Marine Science and Technology (Qingdao) under contract No. 2018SDKJ0505-4; the NSFC-Shandong Joint Funded Project under contract No. U1606404; the UNDP/GEF YSLME Phase II Project.
*Corresponding author, E-mail: zhangxl@fio.org.cn; wangzl@fio.org.cn

2007, 2008) and has increased substantially in the last two decades. Before 2010, the floating *S. horneri* was only reported in the oceanic front between the Kuroshio Current and continental shelf of ECS (Komatsu et al., 2007). Unusual expansion was detected in 2012 when the drifting *S. horneri* rafts were stranded in the northern coast of Taiwan Island and even crossed the Kuroshio Current reaching Tarama Island in the Ryukyu Archipelago (Komatsu et al., 2014). Research using drifting buoys and model simulation suggested that the floating *S. horneri* was originated from the Chinese coasts, presumably from the coasts of Fujian, Zhejiang and Shandong provinces in the YS and ECS (Komatsu et al., 2007; Filippi et al., 2010; Mizuno et al., 2014; Qi et al., 2017). Inundation and stranding events are increasing along the coasts of China and Korea as well (Hu et al., 2011; Liu et al., 2018, 2021; Byeon et al., 2019; Xiao et al., 2020b). In 2015, large amount of floating *Sargassum* stranded and piled up along the southern coastline of Korea (Byeon et al., 2019). In the end of 2016, golden tide in the Subei Shoal at the western coast of southern YS caused over 0.5 billion CNY loss of *Pyropia* cultivation industry. In the following spring and summer 2017, the drifting *S. horneri* rafts were widespread in the western YS and co-occurred with the green tide (Xiao et al., 2020b). Xing et al. (2017) and Qi et al. (2017) traced the floating *S. horneri* back to the coasts of eastern Shandong Peninsula and Zhejiang Province. Although discrete benthic populations were recorded along the eastern coasts of China (Tseng, 1983; Hu et al., 2011; Li et al., 2020), the exact origin of the drifting *S. horneri* in the ECS and YS hasn't been identified and bloom mechanism remains unclear.

Until now, there is no report that floating *S. horneri* can complete their life cycle in the YS and ECS. Previous studies suggested that floating *Sargassum* rafts existed from October to the following July in the YS and ECS and the drifting paths varied in different seasons (Komatsu et al., 2014; Qi et al., 2017; Liu et al., 2018; Su et al., 2018; Xing et al., 2018; Xiao et al., 2020b). To better understand the development and drifting of the golden tide, time series of high-resolution satellite images were used to extract the spatiotemporal distribution of floating *S. horneri* in the YS and ECS throughout a full year period 2019–2020. The pattern of *S. horneri* blooms was characterized and the impacts from temperature and wind field were explored.

2 Data and methods

2.1 *Satellite imageries*

The study area covers waters in the YS and northern ECS, 26°–40°N, 119°–128°E (Fig. 1a). Multi-spectral satellite sensors of Sentinel-2, Gaofen-1/6 (GF-1/6) and Haiyang-1C (H1C) were used in this study (Fig. 2, Table 1). The Sentinel-2 images are provided by European Space Agency; GF-1 and GF-6 images are provided by China Centre for Resources Satellite Data and Application; H1C images are provided by China National Satellite Ocean Application Service. Because thick clouds greatly influence the detection of floating macroalgae from optical images, it is necessary to acquire multi-source images. Sentinel-2 from European Space Agency has a swath width of 290 km, regular revisit frequency of 5 d and high spatial resolution (10 m). Because one time visit of Sentinel-2 cannot fully cover the study area, images obtained 2 d before and after are also included. In this study, we mainly used Sentinel-2 images to quantify the coverage of floating *Sargassum* mats. The only exception was on June 7, 2020, when both Sentinel-2 and GF-1 images was used to gain a whole view of golden tide in the YS and ECS. The wide-field-view (WFV)

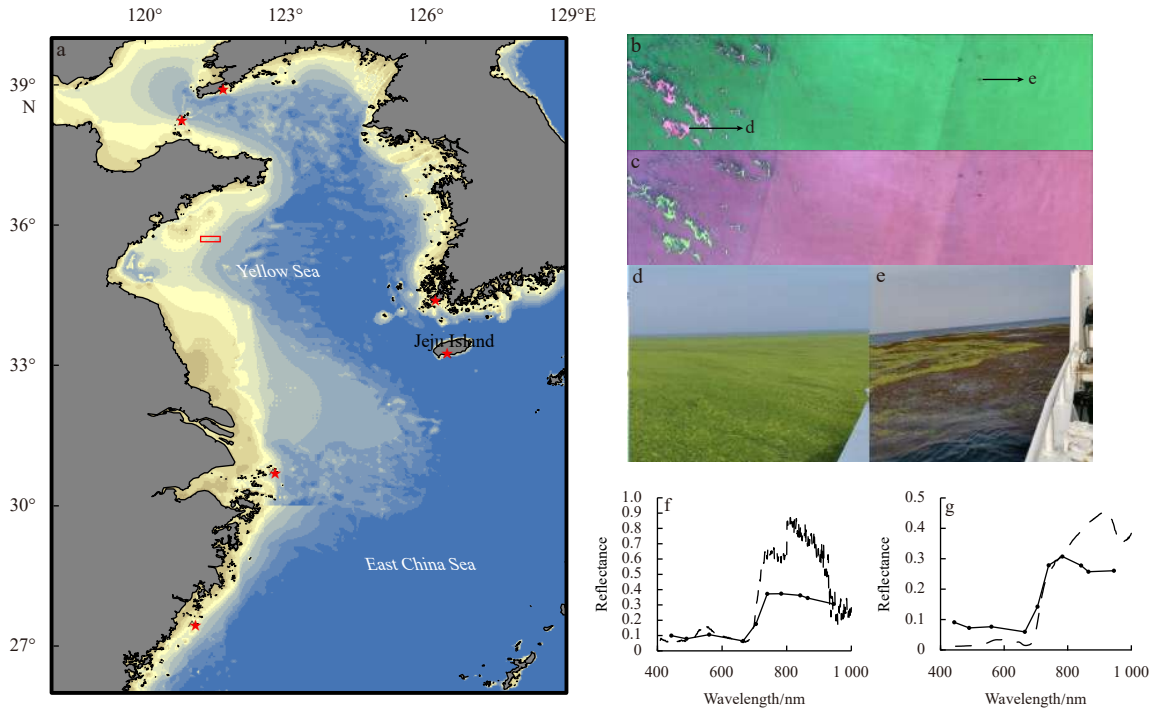

Fig. 1. The bi-macroalgal bloom in the Yellow Sea on June 7, 2020. a. Area covered by the satellite image analysis in the current study. ★ records natural distribution of benthic *Sargassum horneri* in Chinese and Korean waters (Tseng, 1983; Hu et al., 2011; Byeon et al., 2019), □ denotes location of panels b and c; b and c are RED-GREEN-BLUE and NIR-RED-GREEN images from Sentinel-2 satellite; d and e, field validation of green tide caused by *Ulva prolifera* and bloom caused by *Sargassum horneri* from June 7 to 10, 2020, respectively; f and g, reflectance spectrum of *Ulva prolifera* and *Sargassum horneri* from Sentinel-2 MultiSpectral Instrument (solid line with dots) and laboratory measurements (dashed line).

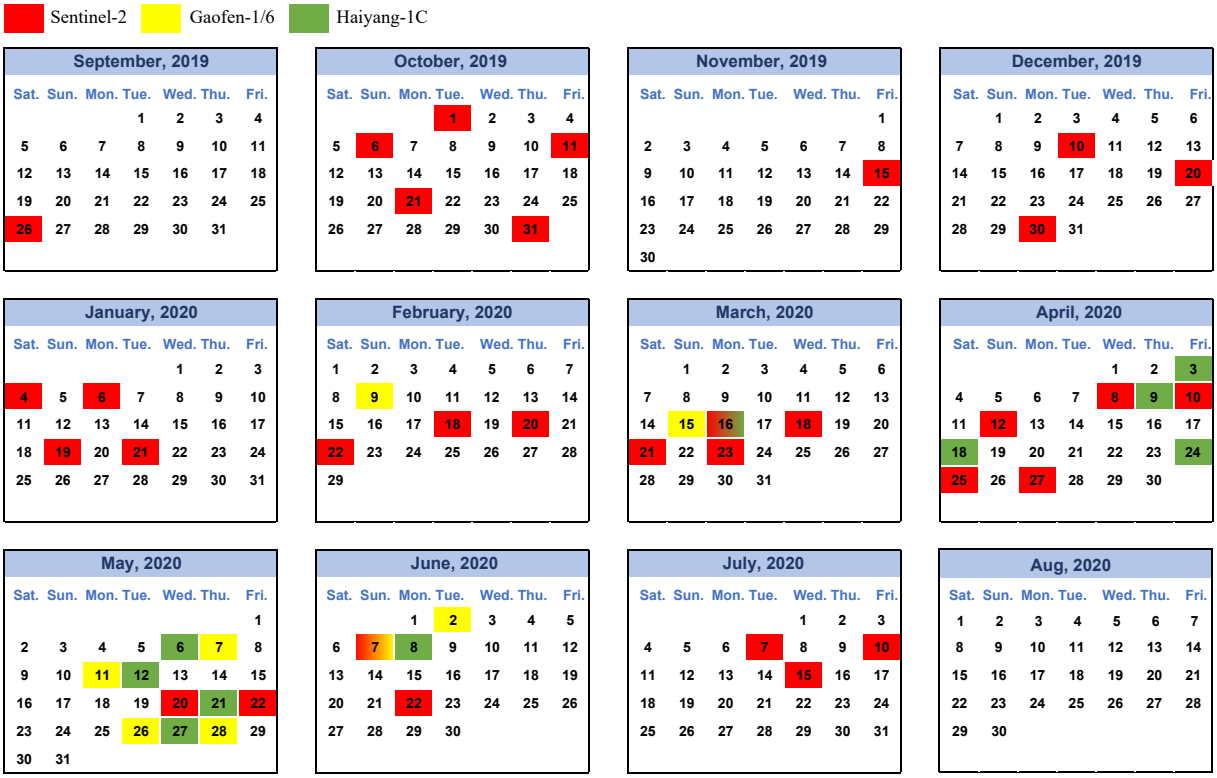

Fig. 2. High resolution images from Sentinel-2 (red), Gaofen-1/6 (yellow) and Haiyang-1C (green) used from September 2019 to August 2020.

Table 1. Sensor characteristics of Sentinel-2, Gaofen-1/6 and Haiyang 1C

Satellite sensor	Sentinel-2 multispectral instrument	Gaofen-1/6 Wide-Field-View	Haiyang 1C Coastal Zone Imager
Blue-Green-Red-Near Infrared Band	2-3-4-8	1-2-3-4	1-2-3-4
Resolution/m	10	16	50
Swath/km	290	800	950
Revisit cycle/d	5	4	3
Data provider	European Space Agency	China Centre for Resources Satellite Data and Application	China National Satellite Ocean Application Service

cameras of GF-1 (and GF-6) have a spatial resolution of 16 m and swath width of 800 km. H1C is launched in September 2018. H1C Coastal Zone Imager (CZI) has a spatial resolution of 50 m and revisits frequency of 3 d. Images from GF-6, GF-1 and H1C were used qualitatively to gain a time-series *Sargassum* distribution patterns in the studied area.

2.2 *Data processing*

The Sentinel-2 Level-2A main output is an orthoimage bottom-of-atmosphere corrected reflectance product (https://sentinels.copernicus.eu/), thus can be directly used for further processing. For GF-6 and GF-1 WFV images, the digital numbers are first converted to radiance according to the calibration coefficients of gain and offsets. The radiance is then transferred to ground reflectance using Fast Line of Sight Atmospheric Analysis of Spectral Hypercubes atmospheric correction.

Sargassum has red-edge spectral characteristics similar to terrestrial vegetation and floating *U. prolifera*. The difference vegetation index (DVI) is used to detect the floating macroalgal rafts. A previous study showed that DVI performed better in reducing the impact of sun glint and thin cloud than normalized DVI (Xing and Hu, 2016). DVI is calculated as

$$\mathrm{DVI} = R_{\mathrm{NIR}} - R_{\mathrm{RED}}, \tag{1}$$

where R_{NIR} and R_{RED} are the surface reflectance of near-infrared and red bands at the ground level, respectively. A threshold of DVI is set to extract the macroalgal pixels, e.g., DVI> –0.008 to 0 for Sentinel-2 images and DVI>–0.010 or –0.015 for GF-6 or GF-1 images. The threshold may be arbitrarily changed slightly depending on surface water optical condition. The coverage area of floating *Sargassum* was calculated from pixels with DVI above the threshold and visual inspection based on RED-GREEN-BLUE (RGB) color composite image (see below for details). The distribution area is manually outlined on each date. The centroids were extracted by the weighted mean centers of positive *Sargassum* pixels' values and connected to gain a general drifting path.

The blooms of *S. horneri* and *U. prolifera* overlapped from May to July. Field samples of *S. horneri* and *U. prolifera* were transported into laboratory. Their reflectance spectra were determined in a blackened tank filled with seawater using an ASD FieldSpec Hand-Held 2 spectrometer. As shown in Fig. 1, both

macroalgae show red color in NIR-RED-GREEN color composite image (Fig. 1c), while *S. horneri* shows (dark) brown and *U. prolifera* is in green color in RGB color composite image, respectively (Fig. 1b). To be more specific, the reflectance spectrum of *U. prolifera* has a peak in green band (~550 nm) while *S. horneri* not (Figs 1f, g). Therefore, we differentiated the distribution of *S. horneri* and *U. prolifera* by their high DVI values together with the RGB color composite images by visual inspection (Xiao et al., 2021a).

The floating *S. horneri* rafts usually have a smaller size than the spatial resolution of pixels (10 m of Sentinel-2 and 16 m of GF-1 and GF-6). For high resolution images, it is reasonable to assume the existence of pixel that was completely covered by macroalgae and its corresponding DVI value was the highest. To solve this subpixel mixing issue, area completely covered by floating *Sargassum* rafts (A_{CCM}) was estimated using a simplified linear-mixing reflectance model from Xing et al. (2017). This model assumed that the portion of macroalgae (POM) in each pixel was linear to the corresponding DVI values normalized to the upper (100%) and lower threshold of DVI values (1%), [01DVI], using Eq. (1). Then, we summed up the POM to calculate A_{CCM} on each date using Eq. (2).

$$\mathrm{POM} = 99 \times [01\mathrm{DVI}] + 1, \tag{2}$$

$$A_{\mathrm{CCM}} = \sum_{i=1}^{n} \mathrm{POM}_i \times \mathrm{PS}_i, \tag{3}$$

where [01DVI] is the normalized DVI for estimating the A_{CCM}. n is the number of pixels containing floating *Sargassum*; PS is the spatial resolution of satellite images, e.g., 10 m×10 m for Sentinel-2 and 16 m×16 m for GF-1/6.

2.3 *Environmental data*

The 9 km Optimal Interpolation Sea Surface Temperature (SST) and Cross-Calibrated Multi-Platform (CCMP) Surface Wind Vectors (0.25°) daily data were obtained from the website of Remote Sensing Systems (www.remss.com). Both data were produced combining multiple satellite sensors, moored buoy and model data. The CCMP daily data were then monthly averaged to obtain the prevailing wind direction. The SST in the *Sargassum* bloom area was extracted and averaged as $\mathrm{SST}_{\mathrm{Sarg}}$.

3 Results

3.1 *The development of Sargassum bloom in the Yellow Sea and East China Sea*

In September 2019, no macroalgal raft was found from Sentinel-2 images. From October 2019 to January 2020, macroalgal rafts were found every month and generally drifted southwards along Chinese coastal waters (Fig. 3a). Floating macroalgae was initially found near the eastern end of Shandong Peninsula on October 21, 2019. In the following month, floating macroalgae moved southwesterly and reached north of Subei Shoal on November 15. On December 10, the floating *Sargassum* rafts arrived at the north edge of *Pyropia* aquaculture area. On January 4, 2020, large amount of *Sargassum* aggregated along the sand grooves and severely damaged the *Pyropia* aquaculture industry. The floating *Sargassum* rafts continued to drift southwards and reached the Changjiang Estuary on January 20.

As shown in Figs 3b and c, another *Sargassum* bloom occurred between the eastern end of Shandong Peninsula and Korean Peninsula on January 20. This bloom was larger in scale than the previous one and mainly distributed in the central YS and northern ECS. The *Sargassum* rafts generally drifted southwards and expanded from January to April, and moved northwards then after until decay in late June. On February 20, floating *Sargassum* rafts were mainly located near the southwest Korean coast and then expanded southwesterly to the central YS and ECS. On March 21, the coverage area of floating *Sargassum* rafts was about 130 km^2 and the southern boundary reached 32°N. One month later, a large area of *Sargassum* could be found in the offshore Zhejiang coast with the southern boundary of 29°N on April 25.

The drifting direction turned northwards from April to May (Fig. 3c). On May 20, golden tide caused by *S. horneri* and green tide caused by *U. prolifera* cooccurred in the YS (Fig. 3c). The Sentinel-2 images indicated that these two macroalgae could be differentiated based on the morphologies and locations of macroalgal rafts. The macroalgal rafts of *S. horneri* tended to scatter separately while *U. prolifera* converged into large patches. On the other hand, the former was mainly distributed in the central YS while the later in coastal waters. From June 7, the coverage area sharply reduced and floating *Sargassum* rafts were mainly distributed in waters west of Jeju Island. On June 22, no obvious signal of floating *Sargassum* rafts was observed in the studied area, indicating the decay of golden tide.

3.2 *Distribution and coverage areas of Sargassum blooms*

In the first drifting path, signals of floating *Sargassum* were weak and clouds always existed over the study area, making it difficult to accurately assess their coverage area. Figure 4 revealed an increase of distribution area from October 2019 to January 2020 in the first drifting path. It should be noted that the distribution area might be underestimated in early January, due to thick clouds persisted between *Pyropia* aquaculture area and Changjiang River Estuary. The timing of highest bloom distribution area arrived earlier than that of peak bloom coverage area. From January to March, in the second drifting path, the distribution area maintained at about 23 000 km^2 while the coverage area increased nearly 40 times (from 3.1 km^2 to 128 km^2). From March to May, the distribution area increased nearly 4 times, while the coverage area decreased slowly to 70 km^2. The maximum distribution area reached 87 500 km^2 on May 20. Linear unmixing models estimated that A_{CCM} were 10.8 km^2, 9.7 km^2 and 7.5 km^2 on March 21, April 25 and May 20, respectively. In June, both distribution and coverage areas of golden tides rapidly declined. No more *Sargassum* bloom were detected in July and August, 2020.

3.3 *Field validation*

Field validation identified the floating brown macroalgae was *S. horneri* (Fig. 5). On January 13, 2020, large amount of *S. horneri* was stranding on the ropes, severely damaging the *Pyropia* aquaculture rafts in the Subei Shoal. From May 17 to 19, visual inspection along the cruise revealed that the floating *Sargassum* rafts scattered in the central YS. The color of *S. horneri* was dark brown in January yet pale yellow in May.

3.4 *Changes of wind field and sea surface temperature (SST)*

We examined the impacts of wind vectors and SST on the development and drifting of floating *Sargassum* in the YS and ECS. Northerly wind prevailed in the floating *Sargassum* bloom areas from late October 2019 to April 2020. From May 2020 to August 2020, the wind direction turned northwards (vectors in Fig. 6). In

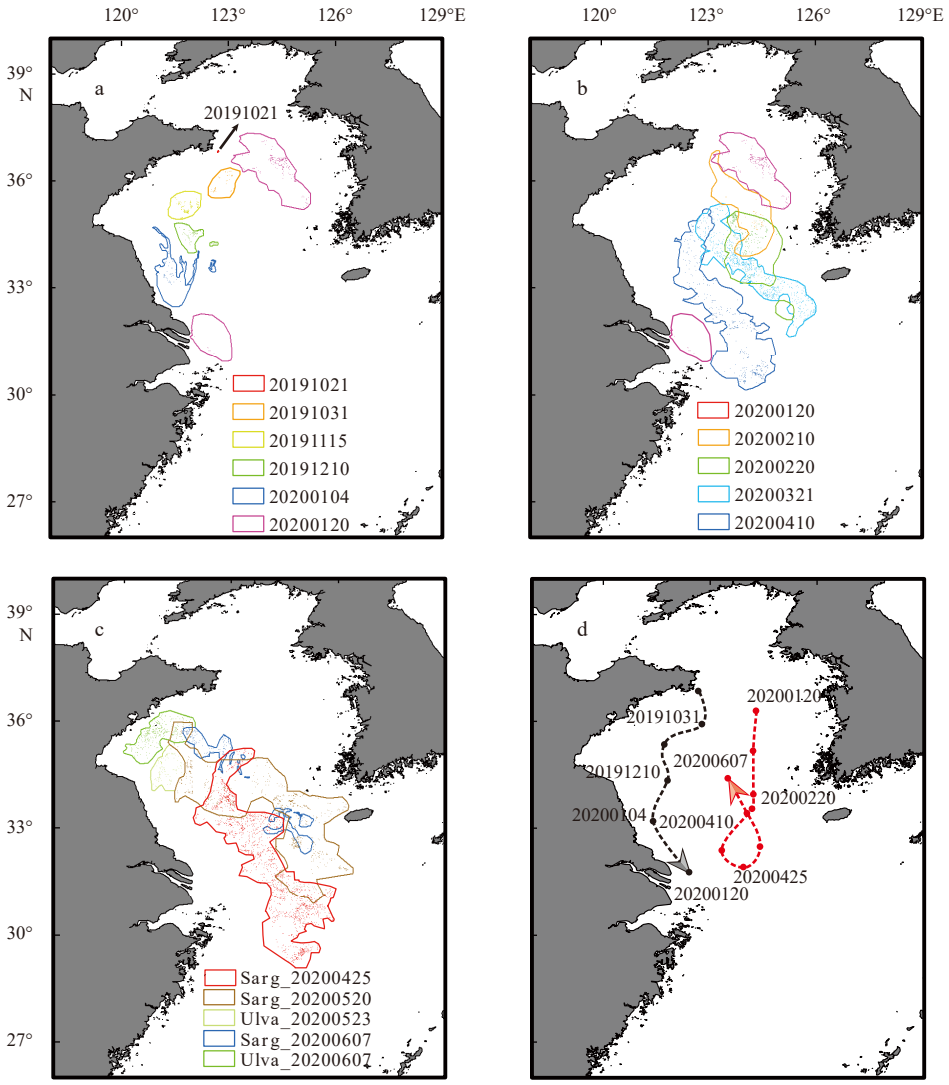

Fig. 3. The distribution area of floating *Sargassum* from October 2019 to January 2020 (a), from January 2020 to April 2020 (b) and from April 2020 to June 2020 (c); two drifting paths of floating *Sargassum* in the Yellow Sea and East China Sea (d). The distribution area on October 21, 2019 is indicated by black arrow in a. Red and black dots indicate the centroids of distribution area on each date (in YYYYMMDD format). The distribution of green tide caused by *Ulva prolifera* was also included in c.

the first drifting path, mean SST for the floating *Sargassum* distribution area (SST_{Sarg}) maintained above 18°C in October and November (contours in Figs 6 and 7). SST_{Sarg} decreased to 14.6°C in December and to 8°C in January, respectively. In the second path, SST_{Sarg} was about 9°C in January, maintained 10–14°C from February to April, increased to 16–17°C on May 20 and reached nearly 20°C on June 7 (contours in Figs 6 and 7).

4 Discussion

Following the green tide caused by *U. prolifera* in the YS, *S. horneri* has been the second macroalgal species forming trans-regional blooms and affecting coastal aquaculture and economy on both sides of the YS and ECS (Komatsu et al., 2007, 2008; Xing et al., 2017; Liu et al., 2018; Byeon et al., 2019; Xiao et al., 2020a). In this study, we investigated the development, distribution and drifting of the *Sargassum* blooms in the YS and ECS throughout the year from September 2019 to August 2020. Two successive blooms were detected in the studied region, one small-scale bloom proceeded in the western YS from October 2019 to January 2020, the other was widely distributed in offshore waters of the South YS and North ECS during January to June 2020. And the drifting and bloom development were found closely associated with the wind trajectory and sea surface temperature. Hereafter, we discussed the characters of *Sargassum* blooms from this study, the differences with previous studies and the possible reasons for these differences, which would assist our understanding the bloom mechanism and future managements of the golden tides in the YS and ECS.

4.1 *Two successive drifting paths of Sargassum blooms*

In the first drifting path, *Sargassum* bloom was detected from late October 2019 to late January 2020. The bloom was onset near the eastern tip of Shandong Peninsula, and expanded through drifting southwards in the following 3 months. This drifting path was consistent with previous results in 2016 (Xing et al., 2017), indicating that the floating *Sargassum* that severely damaged the seaweed aquaculture in Subei Shoal was not from local population, but that originated near the eastern tip of Shandong Penin-

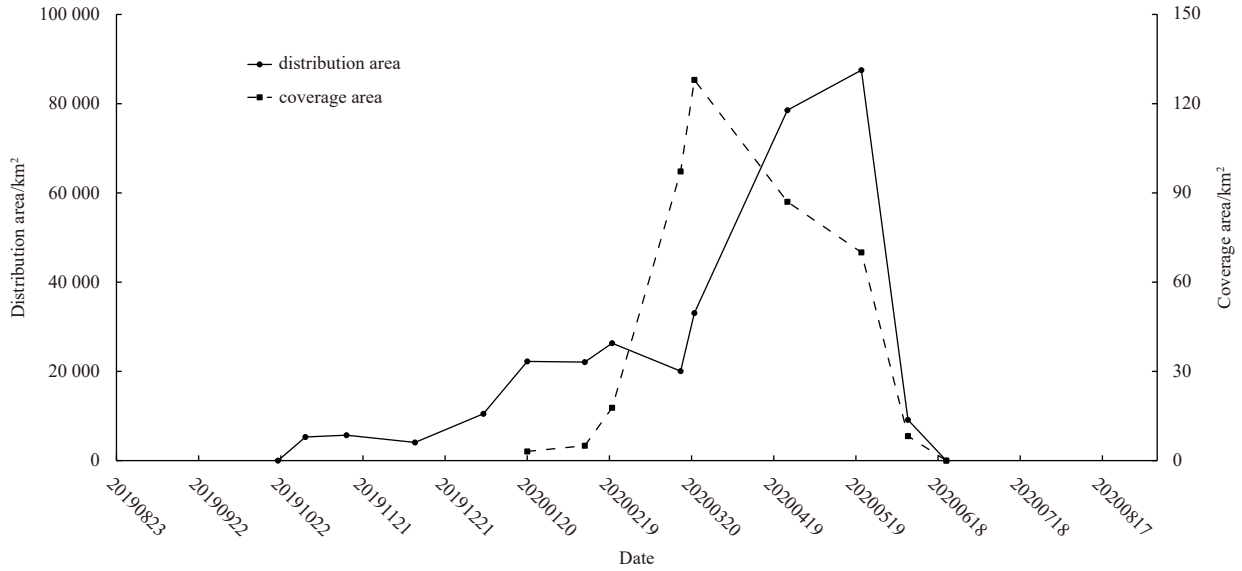

Fig. 4. The distribution and coverage areas of floating *Sargassum* in the Yellow Sea and East China Sea from October 2019 to June 2020 (in YYYYMMDD format).

Fig. 5. Field validation of *Sargassum* bloom in the Subei Shoal on January 14 (a) and in the Yellow Sea on May 19, 2020 (b and c).

sula or north (Fig. 4). In fact, the accumulation of *S. horneri* in the *Pyropia* aquaculture areas has become a normal in recent years (Xiao et al., 2020a; Liu et al., 2021).

The second drifting path lasted 6 months from January to June 2020 and spanned larger spatial scale than the first one. The *Sargassum* blooms were mainly distributed in the central YS and northern ECS and co-occurred with *U. prolifera* green tide in the western YS. The southward drifting path from January to April differed from previous studies based on MODIS and numerical particles simulations. Qi et al. (2017) reported a spring *Sargassum* bloom originated from the offshore Zhejiang coast, transported to the northeast to reach South Korea (Jeju Island) and Japan coastal waters, and then to the northwest to enter the YS by the end of April. This drifting pathway described by Qi et al. (2017) was congruent with the hypotheses from Komatsu et al. (2007, 2008). The southward drifting and expansion in this study suggested that there could be another origin in the YS for the spring blooms beside the one from Zhejiang offshore (Qi et al., 2017). In May, floating *Sargassum* rafts were widely distributed in the central YS and ECS, consistent with previous findings in 2017 (Qi et al., 2017). However, no transportation of floating *Sargassum* from Zhejiang offshore was detected by Sentinel-2 of 10 m spatial resolution in this study.

Tracing back to the origin of *Sargassum* bloom in the YS and ECS is complicated by the wide geographic distribution and huge genetic variation of both floating and benthic *S. horneri* (Hu et al., 2011; Liu et al., 2018; Su et al., 2018; Li et al., 2020). Until now, there is no report that floating *S. horneri* can complete its life cycle in our studies area. Detached *Sargassum* thalli are still considered to be the main source of golden tide (Liu et al., 2018). Due to the scattering characteristics and relatively small scales, it is nearly impossible to identify the source of floating *Sargassum* at its very early stage merely by high resolution images. Nevertheless, our results evidenced that the floating *Sargassum* was mostly likely originated from the north instead of the south of the YS-ECS. Recent years have seen huge amount of *S. horneri* tangling along the *Saccharina* cultivation in Rongcheng at the eastern end of Shandong Peninsula or even in Dalian and Changdao in the northern YS (Liu et al., 2018; Su et al., 2018); Chao Yuan's personal observation). It was possible that these biomasses was manually discarded into the sea due to the serious negative impacts on kelp farming and fisheries. Rafts of floating *S. horneri* might be transported to the south under prevailing wind and current systems. In the southwestern coastline of Korean Peninsula, including Jeju Island, detached biomass of benthic *S. horneri* reached maximum load of 1.6 kg wet weight per square meter from January to March (Choi et al., 2020). Further studies are needed to validate these potential sources' contribution.

4.2 *Development and drifting of Sargassum blooms in relation to environmental factors*

Temperature significantly influences the growth and life cycle of *S. horneri* (Wu et al., 2019), hence the occurrence and decay of *S. horneri* floating blooms. Previous studies reported that *S.*

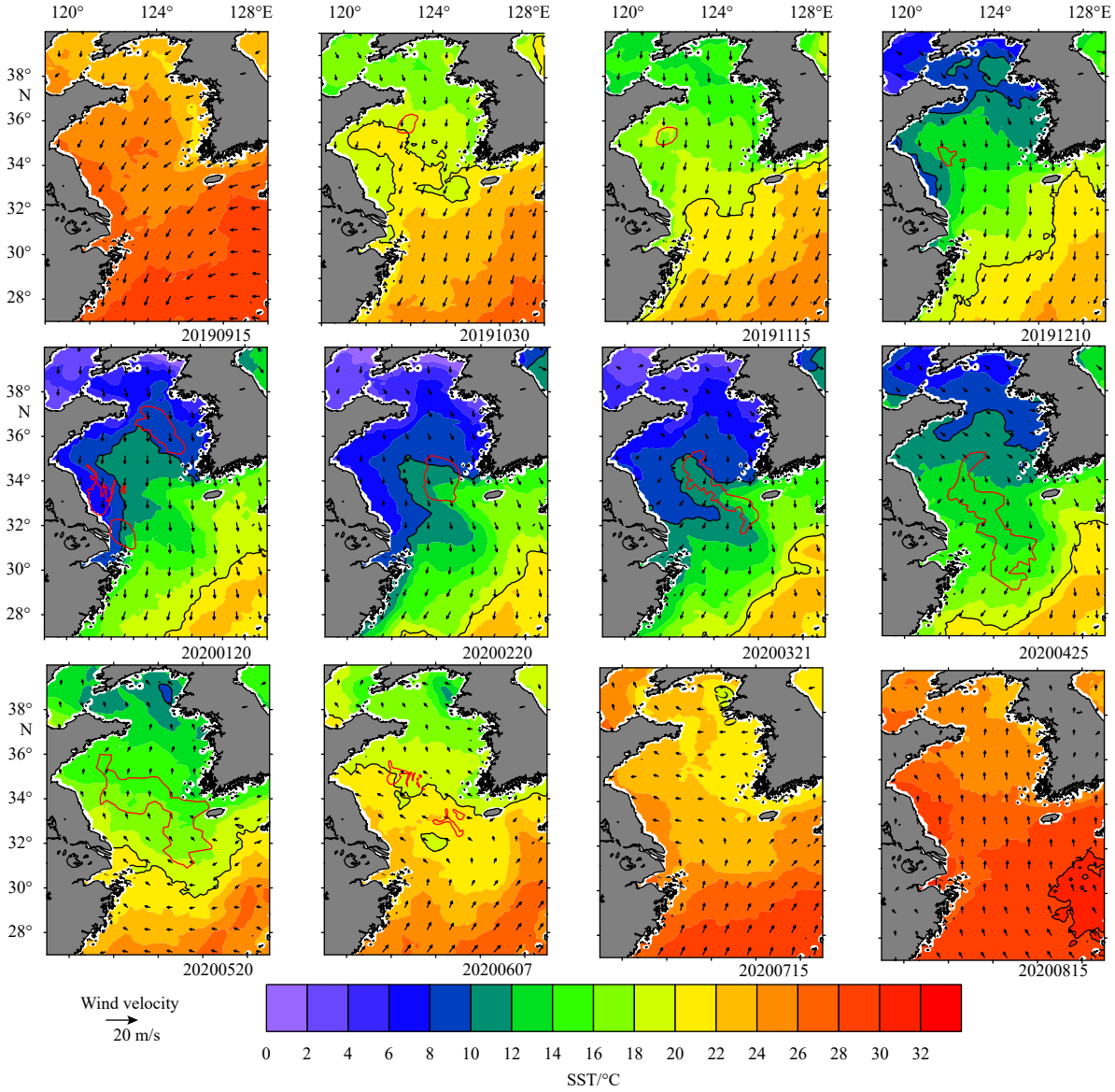

Fig. 6. Distributions of sea surface temperature (contour) and monthly averaged wind field (vectors) in the Yellow Sea and East China Sea from September 2019 to August 2020. The black contour lines indicate 20°C isotherm from 20191030 to 20200607. The distribution of floating *Sargassum* is overlaid in red polygons for each month (in YYYYMMDD format).

horneri can grow over a wide range of temperatures (10–25°C). The optimal growth temperature of *S. horneri* germlings is generally higher than that of adults (25°C vs 15°C) (Mikami et al., 2006; Choi et al., 2009; Pang et al., 2009; Lin et al., 2017). In summer, *S. horneri* germlings or vegetative parts remains are still short (Sun et al., 2008) and the gas vesicles started to emerge in September (Wu et al., 2020). As it takes time for *S. horneri* to gain enough gas vesicles buoyancy to overcome the holdfast，this probably explained that floating bloom was not observed until October (Figs 3 and 4). The SST_{Sarg} from October to December might benefit growth of *S. horneri*. In the second path, the coverage area of Sargassum bloom started with 3.1 km^2 then increased from February to March by 40 times, likely coincident with the increase of SST_{Sarg} from 9.3°C in January to 12.6°C in March (Fig. 7).

Sargassum horneri presents peak sexual reproduction at 16–18°C, after which the germlings sink to the bottom for benthic life stage. On the other hand, more receptacles (Liu et al., 2018) and fewer gas vesicles (Wu et al., 2020) during peak reproduction might make *S. horneri* heavier and sink; even if not sink during reproduction, the adult algae after reproduction will decay (Sun et al., 2008), shed gas vesicles (Xu et al., 2016), lost buoyancy and sink too. Although some floating adult *S. horneri* keep vegetative growth instead of reproduction (Liu et al., 2018), they will cease growth or senesce and lose buoyancy when sea temperature exceeds 20°C (Choi et al., 2009, 2020; Lin et al., 2017). The warming of YS and ECS during June to August 2020 (Fig. 6) matched the above conditions for sinking of *S. horneri*, either adults or germlings. Once sank to waters deeper than 30 m in the central YS and ECS, well below photic zone, *S. horneri* cannot grow or survive to float again. This probably explained the fast decline of floating *S. horneri* in June and vanish during late June to August (Figs 3 and 4). Therefore, floating *S. horneri* is unable to complete life cycle in the YS and ECS. It only blooms in seasons other than summer in the YS and ECS, thus not holopelagic as *S. fluit-*

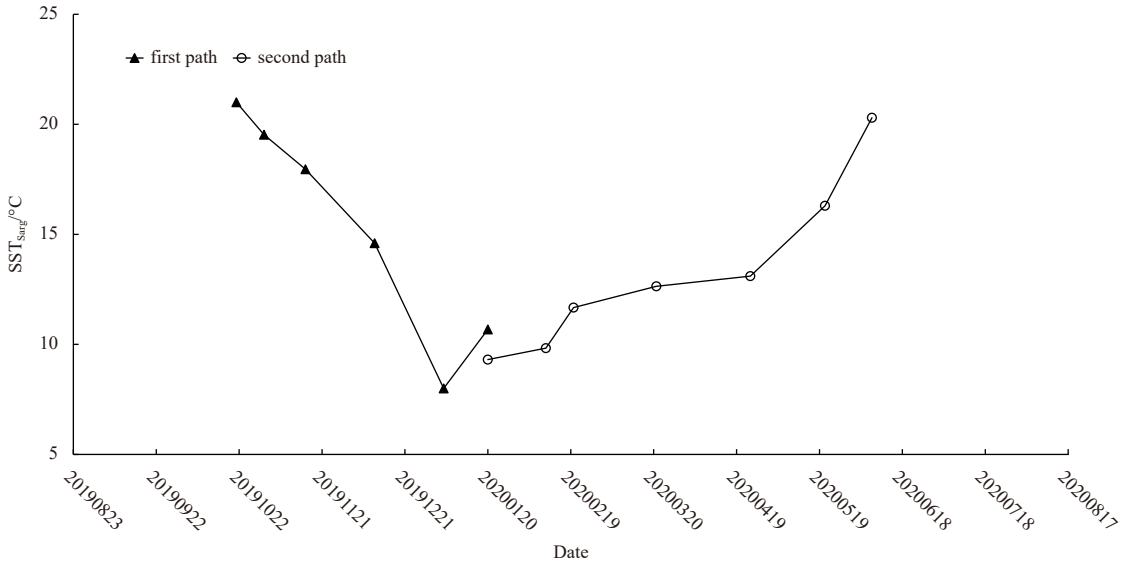

Fig. 7. Temporal variation of sea surface temperature in the areas with *Sargassum* blooms (SST$_{Sarg}$) from October, 2019 to June, 2020 (in YYYYMMDD format).

ans and *S. natans* is in the North Atlantic (Brooks et al., 2018).

Wind vectors and surface currents are two important factors influencing the drifting of floating seaweeds (Liu et al., 2013; Komatsu et al., 2014; Wang et al., 2015, 2019). In 2012, floating *Sargassum* rafts crossed the traditional boundary of Kuroshio Front, and Komatsu et al. (2014) speculated that continuous strong wind and anticyclonic eddy were two important causing factors. In this study, the drifting directions of floating *Sargassum* rafts were generally consistent with the prevailing wind vectors (Fig. 6). The drifting directions of a surface layer generally went at a 45° angle to the wind, indicating the importance of Ekman transport. The drifting directions of floating *Sargassum* rafts seemed to be a balance between the Coriolis force and the drags generated by the winds. When wind directions turned northwards from April 2020, floating *Sargassum* rafts moved into the central YS from the south. Naturally, most part of floating *Sargassum* is submerged below the sea surface, indicating the importance of surface current on their drifting. As observed in the first drifting path (Fig. 3), the drifting directions agreed well with Chinese coastal currents (Xu et al., 2009; Tak et al., 2016). However, the directions were opposite to the northward Yellow Sea Warm Current in the second path, suggesting that winds or wind-driven currents provided stronger drag force.

Our field observations (Fig. 5) confirmed the existence of floating *Sargassum* in our studied area. The changes in pigmentation of *Sargassum* might result from differences in light exposure, physiological states or life stages (Wang et al., 2018). Reduced pigment contents were a common strategy for photosynthetic organisms under high light and floating *Sargassum* were in decay stage in late May, 2020. This also indicated that floating *S. horneri* on different date might have different reflectance. We adopted the normalization of [01DVI] to estimate the A_{CCM}, which could reduce the impact of reflectance changes on different date and was suitable for comparison (Xing et al., 2017).

Management efforts are necessary to mitigate the potential damages of macroalgal blooms. First, high resolution remote sensing is suggested to monitor *Sargassum* blooms and provides information to forecast their development and drifting trend, in order to guide actions before their stranding. Second, strategies are called to remove huge *Sargassum* biomass during the bloom. Assuming a conserved data of 2 kg wet weight *Sargassum* of each square meter bloom area (Mizuno et al., 2014), *Sargassum* biomass was estimated to be 21 600 t during the bloom of peak coverage area. Third, management strategies and actions need to be adapted to the seasonality of *S. horneri* blooms in the YS and ECS, in order to optimize efforts input and maximize effects output.

5 Conclusions

In this study, we found that the seasonal cycle of SST confined the seasonal occurrence of two *Sargassum* blooms in the YS and ECS, one during October–next January and another from January to June. The two *Sargassum* blooms' drifting paths both initiated from around 37°N, firstly moved southwards and corresponded well with prevailing wind field until declined. Floating *S. horneri* cannot complete its life cycle and only blooms in the YS and ECS during seasons other than summer because of warmer SST. The *Sargassum* bloom pattern reported in this study represented a one-year process in the YS and ECS. More extensive studies are needed to validate whether similar pattern exists in other years and to examine the source of these *Sargassum* blooms.

Acknowledgements

We thank Jun Liu from First Institute of Oceanography, Ministry of Natural Resources (MNR) for providing the field photos in Figs 5b and c. We are grateful to staffs in the department of Marine Physics and Remote Sensing, First Institute of Oceanography, MNR for technic supports.

References

Brooks M T, Coles V J, Hood R R, et al. 2018. Factors controlling the seasonal distribution of pelagic *Sargassum*. Marine Ecology Progress Series, 599: 1–18, doi: 10.3354/meps12646

Byeon S Y, Oh H J, Kim S, et al. 2019. The origin and population genetic structure of the 'golden tide' seaweeds, *Sargassum horneri*, in Korean waters. Scientific Reports, 9(1): 7757, doi: 10.1038/s41598-019-44170-x

Choi H G, Lee K H, Yoo H I, et al. 2007. Physiological differences in the growth of *Sargassum horneri* between the germling and

adult stages. In: Borowitzka M A, Critchley A T, Kraan S, et al., eds. Nineteenth International Seaweed Symposium. Dordrecht: Springer, 279–285

Choi S K, Oh H J, Yun S H, et al. 2020. Population dynamics of the 'golden tides' seaweed, *Sargassum horneri*, on the Southwestern Coast of Korea: the extent and formation of golden tides. Sustainability, 12(7): 2903, doi: 10.3390/su12072903

Cui Tingwei, Zhang Jie, Sun Li'e, et al. 2012. Satellite monitoring of massive green macroalgae bloom (GMB): imaging ability comparison of multi-source data and drifting velocity estimation. International Journal of Remote Sensing, 33(17): 5513–5527, doi: 10.1080/01431161.2012.663112

Darling J A, Carlton J T. 2018. A framework for understanding marine cosmopolitanism in the anthropocene. Frontiers in Marine Science, 5: 293, doi: 10.3389/fmars.2018.00293

Fan Shiliang, Fu Mingzhu, Wang Zongling, et al. 2015. Temporal variation of green macroalgal assemblage on *Porphyra* aquaculture rafts in the Subei Shoal, China. Estuarine, 163: 23–28

Filippi J B, Komatsu T, Tanaka K. 2010. Simulation of drifting seaweeds in East China Sea. Ecological Informatics, 5(1): 67–72, doi: 10.1016/j.ecoinf.2009.08.011

Hu Zimin, Uwai S, Yu Shenhui, et al. 2011. Phylogeographic heterogeneity of the brown macroalga *Sargassum horneri* (Fucaceae) in the northwestern Pacific in relation to late Pleistocene glaciation and tectonic configurations. Molecular Ecology, 20(18): 3894–3909, doi: 10.1111/j.1365-294X.2011.05220.x

Komatsu T, Matsunaga D, Mikami A, et al. 2008. Abundance of drifting seaweeds in eastern East China Sea. Journal of Applied Phycology, 20(5): 801–809, doi: 10.1007/s10811-007-9302-4

Komatsu T, Mizuno S, Natheer A, et al. 2014. Unusual distribution of floating seaweeds in the East China Sea in the early spring of 2012. Journal of Applied Phycology, 26(2): 1169–1179, doi: 10.1007/s10811-013-0152-y

Komatsu T, Tatsukawa K, Filippi J B, et al. 2007. Distribution of drifting seaweeds in eastern East China Sea. Journal of Marine Systems, 67(3–4): 245–252

Li Jingjing, Liu Zhengyi, Zhong Zhihai, et al. 2020. Limited genetic connectivity among *Sargassum horneri* (Phaeophyceae) populations in the Chinese Marginal Seas despite their high dispersal capacity. Journal of Phycology, 56(4): 994–1005, doi: 10.1111/jpy.12990

Lin Showe-Mei, Huang Roger, Ogawa H, et al. 2017. Assessment of germling ability of the introduced marine brown alga, *Sargassum horneri*, in Northern Taiwan. Journal of Applied Phycology, 29(5): 2641–2649, doi: 10.1007/s10811-017-1088-4

Liu Dongyan, Keesing J K, Dong Zhijun, et al. 2010. Recurrence of the world's largest green-tide in 2009 in Yellow Sea, China: *Porphyra yezoensis* aquaculture rafts confirmed as nursery for macroalgal blooms. Marine Pollution Bulletin, 60(9): 1423–1432, doi: 10.1016/j.marpolbul.2010.05.015

Liu Dongyan, Keesing J K, He Peimin, et al. 2013. The world's largest macroalgal bloom in the Yellow Sea, China: formation and implications. Estuarine, 129: 2–10

Liu Feng, Liu Xingfeng, Wang Yu, et al. 2018. Insights on the *Sargassum horneri* golden tides in the Yellow Sea inferred from morphological and molecular data. Limnology and Oceanography, 63(4): 1762–1773, doi: 10.1002/lno.10806

Liu Jinlin, Xia Jing, Zhuang Minmin, et al. 2021. Golden seaweed tides accumulated in *Pyropia* aquaculture areas are becoming a normal phenomenon in the Yellow Sea of China. Science of the Total Environment, 774: 145726, doi: 10.1016/j.scitotenv.2021.145726

Marks L, Salinas-Ruiz P, Reed D, et al. 2015. Range expansion of a non-native, invasive macroalga *Sargassum horneri* (Turner) C. Agardh, 1820 in the eastern Pacific. BioInvasions Records, 4(4): 243–248, doi: 10.3391/bir.2015.4.4.02

Masaki H. 2007. Settlement of germlings in some Japanese sargassaceae. Sessile Organisms, 24(2): 89–94, doi: 10.4282/sosj.24.89

Mikani A, Komatsu T, Aoki M, et al. 2006. Seasonal changes in growth and photosynthesis-light curves of *Sargassum horneri* (Fucales, Phaeophyta) in Oura Bay on the Pacific coast of central Honshu, Japan. La Mer, 44(3–4): 109–118

Mizuno S, Ajisaka T, Lahbib S, et al. 2014. Spatial distributions of floating seaweeds in the East China Sea from late winter to early spring. Journal of Applied Phycology, 26(2): 1159–1167, doi: 10.1007/s10811-013-0139-8

Pang Shaojun, Liu Feng, Shan Tifeng, et al. 2009. Cultivation of the brown alga *Sargassum horneri*: sexual reproduction and seedling production in tank culture under reduced solar irradiance in ambient temperature. Journal of Applied Phycology, 21(4): 413–422, doi: 10.1007/s10811-008-9386-5

Qi Lin, Hu Chuanmin, Wang Mengqiu, et al. 2017. Floating algae blooms in the East China Sea. Geophysical Research Letters, 44(22): 11501–11509, doi: 10.1002/2017GL075525

Smetacek V, Zingone A. 2013. Green and golden seaweed tides on the rise. Nature, 504(7478): 84–88, doi: 10.1038/nature12860

Song Wei, Li Yan, Fang Song, et al. 2015a. Temporal and spatial distributions of green algae micro-propagules in the coastal waters of the Subei Shoal, China. Estuarine, 163: 29–35

Song Wei, Peng Keqin, Xiao Jie, et al. 2015b. Effects of temperature on the germination of green algae micro-propagules in coastal waters of the Subei Shoal, China. Estuarine, 163: 63–68

Su Li, Shan Tifeng, Pang Shaojun, et al. 2018. Analyses of the genetic structure of *Sargassum horneri* in the Yellow Sea: implications of the temporal and spatial relations among floating and benthic populations. Journal of Applied Phycology, 30(2): 1417–1424, doi: 10.1007/s10811-017-1296-y

Sun Jianzhang, Chen Wandong, Zhuang Dinggen, et al. 2008. *In situ* ecological studies of the subtidal brown alga *Sargasssum horneri* at Nanji Island of China. South China Fisheries Science (in Chinese), 4(3): 58–63

Tak Y J, Cho Y K, Seo G H, et al. 2016. Evolution of wind-driven flows in the Yellow Sea during winter. Journal of Geophysical Research: Oceans, 121(3): 1970–1983, doi: 10.1002/2016JC011622

Tseng C K. 1983. Common Seaweeds of China. Beijing: Science Press

Wang Mengqiu, Hu Chuanmin, Barnes B B, et al. 2019. The great atlantic *Sargassum* belt. Science, 365(6448): 83–87, doi: 10.1126/science.aaw7912

Wang Mengqiu, Hu Chuanmin, Cannizzaro J, et al. 2018. Remote sensing of *Sargassum* biomass, nutrients, and pigments. Geophysical Research Letters, 45(22): 12359–12367, doi: 10.1029/2018GL078858

Wang Zongling, Xiao Jie, Fan Shiliang, et al. 2015. Who made the world's largest green tide in China?—an integrated study on the initiation and early development of the green tide in Yellow Sea. Limnology and Oceanography, 60(4): 1105–1117, doi: 10.1002/lno.10083

Wu Zuli, Chen Liangran, Wang Kai, et al. 2020. Morphological characteristics of vesicle of *Sargassum horneri* and its relationship to environmental factors in Gouqi Island. Journal of Fisheries of China (in Chinese), 44(5): 793–804

Wu Hailong, Feng Jingchi, Li Xinshu, et al. 2019. Effects of increased CO_2 and temperature on the physiological characteristics of the golden tide blooming macroalgae *Sargassum horneri* in the Yellow Sea, China. Marine Pollution Bulletin, 146: 639–644, doi: 10.1016/j.marpolbul.2019.07.025

Xiao Jie, Fan Shiliang, Wang Zongling, et al. 2020a. Decadal characteristics of the floating *Ulva* and *Sargassum* in the Subei Shoal, Yellow Sea. Acta Oceanologica Sinica, 39(10): 1–10, doi: 10.1007/s13131-020-1655-4

Xiao Yanfang, Liu Rongjie, Kim K, et al. 2021a. A random forest-based algorithm to distinguish *Ulva prolifera* and *Sargassum* from multispectral satellite images. IEEE Transactions on Geoscience and Remote Sensing, 60: 4201515, doi: 10.1109/TGRS.2021.3071154

Xiao Jie, Wang Zongling, Liu Dongyan, et al. 2021b. Harmful macroalgal blooms (HMBs) in China's coastal water: green and golden tides. Harmful Algae, 107: 102061, doi: 10.1016/j.hal.2021.102061

Xiao Jie, Wang Zongling, Song Hongjun, et al. 2020b. An anomalous bi-macroalgal bloom caused by *Ulva* and *Sargassum* seaweeds during spring to summer of 2017 in the western Yellow Sea,

China. Harmful Algae, 93: 101760, doi: 10.1016/j.hal.2020.101760

Xing Qianguo, Guo Ruihong, Wu Lingling, et al. 2017. High-resolution satellite observations of a new hazard of golden tides caused by floating *Sargassum* in winter in the Yellow Sea. IEEE Geoscience and Remote Sensing Letters, 14(10): 1815–1819, doi: 10.1109/LGRS.2017.2737079

Xing Qianguo, Hu Chuanmin. 2016. Mapping macroalgal blooms in the Yellow Sea and East China Sea using HJ-1 and Landsat data: application of a virtual baseline reflectance height technique. Remote Sensing of Environment, 178: 113–126, doi: 10.1016/j.rse.2016.02.065

Xing Qianguo, Wu Lingling, Tian Liqiao, et al. 2018. Remote sensing of early-stage green tide in the Yellow Sea for floating-macroalgae collecting campaign. Marine Pollution Bulletin, 133: 150–156, doi: 10.1016/j.marpolbul.2018.05.035

Xu Min, Sakamoto S, Komatsu T. 2016. Attachment strength of the subtidal seaweed *Sargassum horneri* (Turner) C. Agardh varies among development stages and depths. Journal of Applied Phycology, 28(6): 3679–3687, doi: 10.1007/s10811-016-0869-5

Xu Lingling, Wu Dexing, Lin Xiaopei, et al. 2009. The study of the Yellow Sea Warm Current and its seasonal variability. Journal of Hydrodynamics, Ser. B, 21(2): 159–165

Yoshida T. 1963. Studies on the distribution and drift of the floating seaweeds. Bulletin of Tohoku Regional Fisheries Research Laboratory, 23: 141–186